J Appl Electrochem (2008) 38:965–971
DOI 10.1007/s10800-008-9507-5

ORIGINAL PAPER

Cavity microelectrodes for the voltammetric investigation of electrocatalysts: the electroreduction of volatile organic halides on micro-sized silver powders

Alberto Vertova · Rachid Barhdadi · Christine Cachet-Vivier · Cristina Locatelli · Alessandro Minguzzi · Jean-Yves Nedelec · Sandra Rondinini

Received: 13 September 2007 / Revised: 31 January 2008 / Accepted: 31 January 2008 / Published online: 14 February 2008

Abstract In this work the use of cavity-microelectrodes is described for the study of the electrocatalytic properties of silver powders in the electroreduction of trichloromethane, taken as model compound. The key role played by the Ag surface status has driven the research towards the use of micro- and nanosized materials, whose exploitation requires the full understanding of the complex behaviour of multiphasial interfaces, and the development of the appropriate investigation methodologies. Moreover, comparison with electrodeposited silver macroelectrodes demonstrates the advantages of using cavity-microelectrodes, especially in terms of improvement of the electrocatalytic activity, insignificance of ohmic drop and double layer capacitance in the voltammetric response, and simplicity offered by the experimental procedure for renovating the electrode material and surface.

Keywords Electrocatalysis · Silver · Volatile organic halides · Trichloromethane · Microelectrode

1 Introduction

Volatile organic halides (VOH) are a large family of substances, among which the more ubiquitous compounds are chlorinated solvents like CH_2Cl_2 (pharmaceuticals, chemical processing, aerosols, etc.), $CHCl_3$, CCl_4, $Cl_2C{=}CCl_2$ (dry and metal cleaning), and $Cl_2C{=}CHCl$ (metal cleaning and specialty adhesives). Notwithstanding their relatively short atmospheric life-time [1] (e.g. 6–8 days for trichloroethylene and 5–6 months for tetrachloroethylene and dichloromethane), their toxicity together with the wide spectrum of waste types (from concentrated organic solutions/emulsions to very dilute aqueous phases, to airborne streams) constitute serious challenges in developing suitable treatment methodologies. Despite the several biological and physico-chemical methods proposed so far, none of them is free from some significant drawback, e.g. formation of undesirable by-products, excess of reagent, exhaustion of absorbing substrates, which require additional treatment steps.

On account on their higher selectivity, milder reaction conditions and simpler process design and operation, electrochemical methods can play a key role in environmental protection and remediation.

Although electrooxidative processes are more attractive, because they may lead to the complete mineralization of the substrate, and have been therefore more studied [2], their application to VOH degradation may produce undesired chlorinated compounds possibly even more toxic than the treated substrates. On the other hand, the electroreductive route, leading to hydrodehalogenated derivatives (e.g. CH_4, C_2H_6, C_2H_4), represents a convenient way of waste detoxification, provided that the dehalogenation is exhaustive.

In this context the highly electrocatalytic properties of silver towards organic halide electroreductions [3–8] have been successfully applied to VOH degradations [9, 10]. In particular the electroreduction of $CHCl_3$ in non-aqueous and aqueous media has been shown to give CH_4 as main product [9, 10].

A. Vertova (✉) · C. Locatelli · A. Minguzzi · S. Rondinini
Department of Physical Chemistry and Electrochemistry, The University of Milan, via Golgi 19, 20133 Milan, Italy
e-mail: alberto.vertova@unimi.it

R. Barhdadi · C. Cachet-Vivier · J.-Y. Nedelec
Electrochimie et Synthèse Organique, Institut de Chimie et des Matériaux Paris Est, UMR 7182 CNRS-Université Paris Val de Marne, 2 Rue H. Dunant, 94320 Thiais, France

This remarkable behaviour of silver allows the development of low specific energy consumption processes, thanks to the concomitant reduction of cell voltage and increase in current efficiency and substrate conversion. It is assumed to be linked with the well-known specific interactions of silver with halide anions [11–14], which, in turn, are governed by the Ag surface state and its modifications in dependence on the composition of the reaction medium (i.e. the halide leaving group, the structure of the organic moiety, the solvent and the supporting electrolyte). In particular, the electrocatalytic activity of silver was reported to increase with increasing surface roughness [15, 16], thus prompting the research toward the development of micro- and nano-sized electrode materials, whose properties usually encompass the simple geometric effect on the real surface area. New investigation methodologies have to be developed, which allow easy separation between the different contributions of the disperse electrocatalytic material and its immobilizing system.

Although the development of solid electrodes with high surface area [17, 18] is frequently treated in the literature, to the author's best knowledge the use of silver in dispersed form as electrocatalyst for chlorinated product remediation has not been reported so far.

In the present work we investigate the electrocatalytic activity of micro-sized silver powders toward the model electroreduction of trichloromethane in non-aqueous medium by using the cavity microelectrode (C-ME) [19–22].

C-ME's are greatly attractive because of their low impact on the supported materials (neither special manipulations nor sticking agents are required) and of the offered possibility of quick and reliable renovation of the electrode surface by a rather simple operation of emptying-and-reloading with fresh material.

In our study, the voltammetric behaviour of the C-ME filled with commercially available micro-sized silver powders will be compared to the one of polycrystalline silver micro-particles electrodeposited onto Pt disks (3 mm diameter). These deposits were obtained using both $KAg(CN)_2$ and $AgNO_3$ baths, at a current density (5 mA cm^{-2}) ten times larger than the one used in most of the previous studies [3–6, 9, 15]. Although it is well known that the silver deposit grown from silver nitrate bath tends to be dendritic, the replacement of the cyanide bath was prompted by both environmental considerations and the need of avoiding any cyanide contamination in the final deposit. In fact, studies on electrodeposited gold from cyanide baths showed that the cyanide can be inglobated within the deposit [23], and work is in progress to confirm possible similarities in the silver deposits. In the following, the electrochemical results for the two new deposits and for the powder electrode will be compared to that of Ag electrodeposited at 0.5 mA cm^{-2} from cyanide bath described in previous work [9, 10].

2 Experimental

2.1 Preparation of the cavity microelectrodes (C-ME)

The C-ME were prepared as previously described [19, 20] from a Pt wire of 50 μm diameter, with typical depths of 20–30 μm. The formation of the recess was followed by optical microscope (Olympus BX30) until the desired depth, L (μm), was reached within an uncertainty of ±2 μm, corresponding to a division of the micrometric screw.

The exact value was obtained by measuring the steady state reduction current in $Ru(NH_3)_6Cl_3$ 1 mM solution (using aqueous KCl 0.1 M as supporting electrolyte) at 1 mV s^{-1} and solving for L Eq. 1, relevant to planar diffusion in a recess [24]:

$$I_l = \frac{4\pi n F c_b D r^2}{4L + \pi r} \quad (1)$$

were I_l is the steady state current intensity, L and r are cavity depth and nominal radius respectively, c_b and D are the Ru(III) complex concentration and diffusion coefficient, respectively, F the Faraday constant.

The cavity was filled with material particles using the electrode as a pestle. The filling of the cavity was controlled with the microscope, and at the same time, it was verified that no particle remained on the head outside the cavity. In this work a commercial microcrystalline Ag powder was used (Aldrich, 99.9%, nominal particle mean diameter 2–3.5 μm). C-ME containing Ag will be denoted Ag_powder. At the end of each experiment, the cavity was emptied by sonicating (Ultrasonic Falck UTD18) the electrode dipped in concentrated HNO_3 aqueous solution (10′) and then in acetonitrile (2′). The cavity was then dried at 80 °C.

2.2 Preparation of electrodeposited Ag

A 3 mm diameter Pt disk, embedded in a PTFE matrix, was covered with silver by cathodic deposition against a silver anode from either 0.05 M $KAg(CN)_2$ or 0.1 M $AgNO_3$ aqueous solutions, at 5 mA cm^{-2} for 18 min (electrodes Ag_CN_high and Ag_NO3_high). Before the deposition, the surface was cleaned using sandpaper (2,400 and 4,000 mesh) and, subsequently, Al_2O_3 water slurry (medium particle diameter: 0.05 and 0.03 μm). The deposit homogeneity was checked using a Wild Photomakroskop M400 optical microscope.

2.3 Cyclic voltammetry (CV)

Voltammetric investigations were carried out using an AMEL 5000 potentiostat/galvanostat driven by Corrware Scribner Associates Inc.

The electrolyte solution consisted of HPLC grade acetonitrile (MeCN, Merck ≥99.8%) containing tetraethylammonium tetrafluoborate (TEATFB, Aldrich ≥99.8%) 0.1 M. An aqueous saturated calomel electrode (SCE) and a platinum foil were used as the reference and counter electrodes respectively. CVs were always first performed on background electrolyte. The desired trichloromethane concentrations were obtained by adding appropriate amounts of 0.5 M $CHCl_3$ (Merck ≥99.8%) in MeCN. Before any recording the solutions were deaerated by nitrogen bubbling. All potentials are referred to SCE.

2.4 Scanning electron microscopy (SEM) pictures

Scanning Electron Microscopy (SEM) photographs were acquired with a LEO 1430 (Ag_NO3_high) and with a Leica Stereoscan 440 (commercial microcrystalline Ag powder).

3 Results

3.1 Electrodeposited silver

Figure 1 compares the CVs of 1.3 mM trichloromethane, in TEATFB 0.1 M in MeCN, recorded at the same scanning rate (500 mV s^{-1}) on Ag_CN_high and Ag_NO3_high respectively obtained by electrodeposition at 5 mA cm^{-2} from cyanide and nitrate baths (curves a and b, present work), and on Ag_CN_low obtained at 0.5 mA cm^{-2} from cyanide bath (curve c, from previous work [9] in $c_{CHCl_3} = 2$ mM, rescaled for the sake of comparison).

Up to three peaks are observed, grouped in the −1.2/−1.6 V (group 1 in Fig. 1) and in the −2.1/−2.3 V (group 2, in Fig. 1) ranges. The two groups are reasonably assigned to consecutive reactions, namely from $CHCl_3$ to CH_2Cl_2 and from CH_2Cl_2 to CH_3Cl, respectively, while the differences in peak number and position within each group highlight the critical role played by the silver surface and specifically interacting anions.

In particular, curves b and c show one peak (1a in Fig. 1) at −1.3 and −1.2 V, respectively, which is absent in curve a. These features are further modified in the subsequent cycles, the more evident change being the disappearance of peak 1a in all CVs. We suggest that this peak is linked with the most active silver surface sites

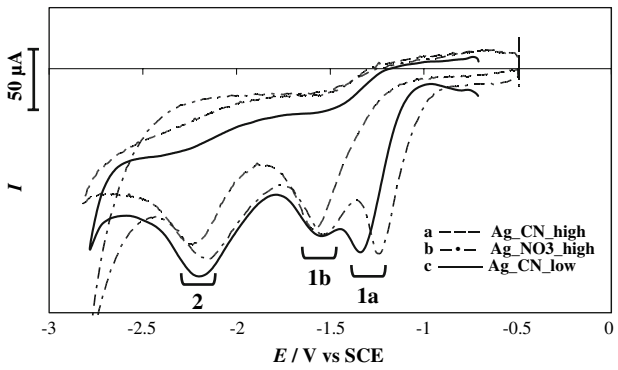

Fig. 1 CV characteristics (1st cycle) on Pt electrode coated with Ag electrolytic deposit, in TEATFB 0.1 M in MeCN, $v = 500$ mV s^{-1}: (a) Ag_CN_high (dashed line), $c_{CHCl_3} = 1.3$ mM;(b) Ag_NO3_high (dash-and-dot line), $c_{CHCl_3} = 1.3$ mM; (c) Ag_CN_low (solid line, from [9] rescaled for the sake of comparison), $c_{CHCl_3} = 2$ mM

which are easily saturated by competing adsorbing species like the leaving chlorides, possible reaction intermediates and/or residual cyanides [15]. For example, the adsorption of cyanides on the same $CHCl_3$ reacting sites could account for the striking difference in the behaviour of Ag_CN_high and Ag_CN_low (compare curves a and c). The possible inclusion of cyanide species during the electrodeposition of silver and its dependence on current density is currently under investigation.

To demonstrate the presence of reaction sites having different electrocatalytic activity, the substrate concentration was progressively reduced. The evolution of CVs (first cycle) with $CHCl_3$ concentration on Ag_CN_high is shown in Fig. 2. All curves have two peak regions 1b and 2. For intermediate concentrations (0.67 and 1 mM), the peak 1b splits into two components at −1.5 and −1.7 V. This phenomenon is even more evident in the subsequent cycles, as in the case of Fig. 3 for the 0.67 mM $CHCl_3$ solution. At the lowest concentration ($c_{CHCl_3} = 0.33$ mM), only the

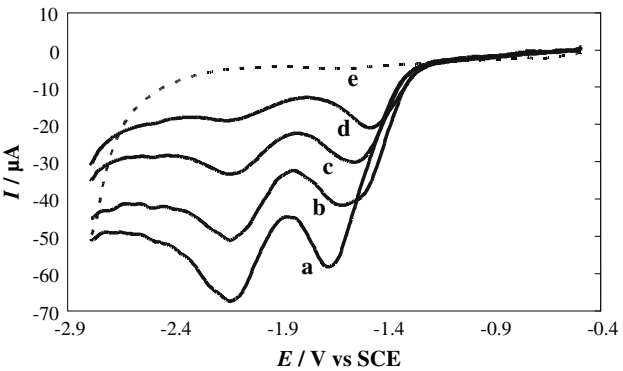

Fig. 2 CV characteristics (1st cycle) of Ag_CN_high, in TEATFB 0.1 M in MeCN, $v = 100$ mV s^{-1}, containing $CHCl_3$ at (a) 1.3 mM, (b) 1 mM, (c) 0.67 mM, (d) 0.33 mM. Line (e) represents background electrolyte. The reverse scan has been omitted for the sake of clarity

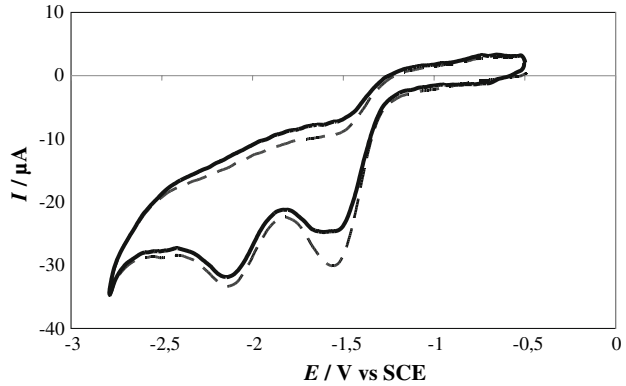

Fig. 3 CV characteristics of Ag_CN_high, in TEATFB 0.1 M in MeCN, $v = 100$ mV s^{-1}, containing 0.67 mM $CHCl_3$. First cycle (dashed line) and "steady-state" cycle (solid line)

component at −1.5 V is observed whereas at the highest concentration ($c_{CHCl_3} = 1.3$ mM) only the component at −1.7 V is visible. The presence of a less negative peak at lower concentrations is consistent with the weak adsorption of reaction products/intermediates. The potential of the peak at around −2.1 V is almost independent on $CHCl_3$ concentration.

When considering the CV characteristics recorded on Ag_NO3_high (see Fig. 4, 1st cycle) the three peaks 1a, 1b and 2 are observed for all $CHCl_3$ concentrations. All the peak currents vary linearly with substrate concentration. Beside the analytical implications, this represents an indirect proof of the stability of the deposit, which, due to the short deposition time, is far from being dendritic (see Fig. 5), but rather appears as formed of compact and dispersed grains the sizes of which are between 10 and 30 µm.

In terms of potentials, peak 1a is independent of concentration, while, again, peak 1b shifts and broadens as for the case of Ag_CN_high. Moreover, peak 1a disappears in the subsequent cycles and also in the case of consecutive

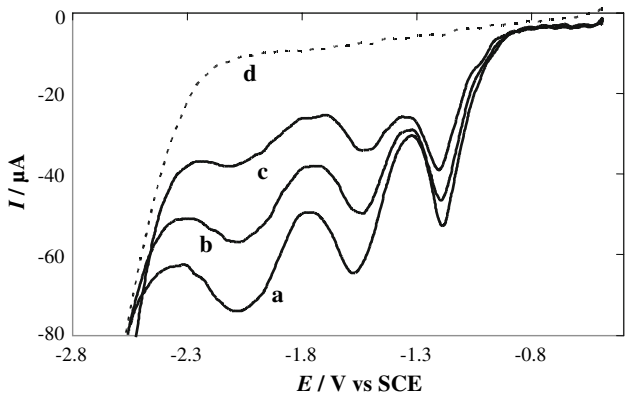

Fig. 4 CV characteristics (1st cycle) of Ag_NO3_high, in TEATFB 0.1 M in MeCN, $v = 100$ mV s^{-1}, containing $CHCl_3$ at (a) 1.3 mM, (b) 1 mM, (c) 0.67 mM. Line (d) represents background electrolyte. The reverse scan has been omitted for the sake of clarity

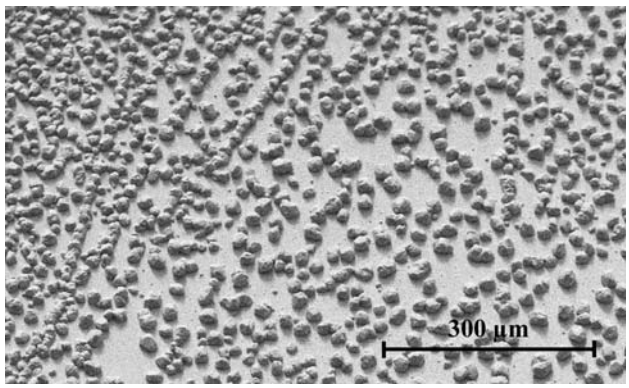

Fig. 5 SEM image of the Ag_NO3_high electrode

recordings, unless the electrode is allowed to rest in the solution at open circuit, possibly denoting slow depoisoning of the silver surface.

Figure 6 collects the curves obtained on the same electrode in the following sequence: (a) first use; (b) recorded immediately after (a); from (c) to (f) recorded after rest at open circuit, until specific open circuit potentials (OCP) are reached, for (f) 1st and 2nd cycles are shown. To follow the electrode depolarization and the surface depoisoning processes, OCPs are more reliable than resting times, which in turn ranged from few minutes to about 1 h.

In the case of curve (b) (for which an OCP value of −0.95 V is observed), only the more negative component of peak 1b is still present showing that the reaction occurs through a modified surface layer (e.g. by adsorbates like possible reaction intermediates and/or chloride leaving

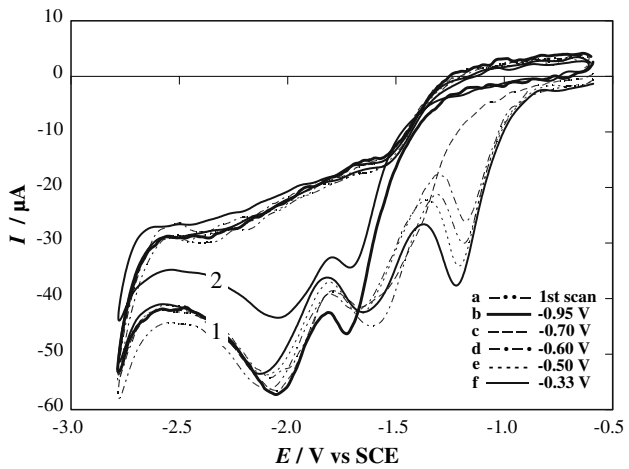

Fig. 6 CV characteristics of Ag_NO3_high, in TEATFB 0.1 M in MeCN, $v = 100$ mV s^{-1}, containing 2.5 mM $CHCl_3$. (a) First scan (dash-dot-dot line) after $CHCl_3$ addition; subsequent scans, recorded after rest at open circuit condition, until the OCP reaches: (b) (thick solid line) −0.95 V; (c) (dashed line) −0.70 V; (d) (dash-and-dot line) −0.60 V; (e) (dotted line) −0.50 V; and (f) (thin solid line) −0.33 V, 1st and 2nd cycles. 1 and 2 denote 1st and 2nd cycles

groups). Peak 1a reappears when the OCP reaches a value around −0.6 V, the peak current slowly increasing with increasing OCP values. This is consistent with the progressive restoring of free Ag sites by desorption of interacting species. Concomitantly, peak 1b broadens revealing the presence of a pre-peak as discussed in Figs. 2 and 3. Any subsequent cycle (here reported for curve f only) is independent on the rest period and is similar to curve (b) but with reduced current values.

Comparing the results obtained on Ag_CN_high and Ag_NO3_high, the superior performance of the latter kind of electrodes is evident, which shows the accessibility of very active surface sites and their possible restoration.

In view of the role played by the surface and its roughness, the CV analysis was extended to microcrystalline Ag powders, whose characterization required the use of C-ME as supporting electrodes, as described in the next section.

3.2 Micro-sized silver (C-ME)

The use of C-ME required some preliminary experiments to establish the most effective operating procedure.

The main problem encountered in using C-ME supported Ag powders is the presence of dissolved oxygen, which is hard to remove from the cavity. Simple N_2 bubbling, even for extended time, was unsuccessful. A polarization step at −2 V for 5 min, before adding the substrate, proved effective, and to provide the background characteristics of double-layer charging (see Fig. 7). Very likely, this procedure is also effective for the reduction of any possible form of surface silver oxide.

The filling of the cavity was highly reproducible; a maximum difference of 9% was observed in the peak current for repeated electrode filling/emptying procedures.

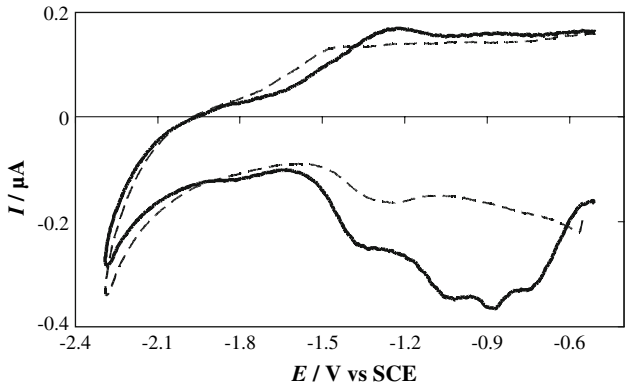

Fig. 7 CV characteristics (1st cycle) of Ag_powder, in TEATFB 0.1 M in MeCN, $v = 2{,}000$ mV s^{-1}: (solid line) after 30 min N_2 bubbling; (dashed line) after polarization at −2 V for 5 min

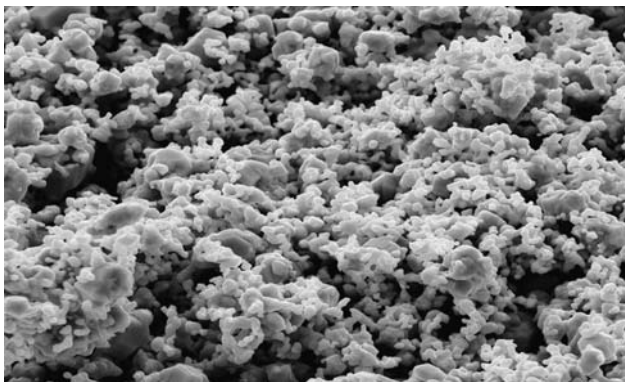

Fig. 8 SEM image of the micro-sized Ag powder

To this end, the cavity size was tailored to the particle size of the commercial Ag powder (see Fig. 8).

As predicted by the theory, the C-ME behaves as a microelectrode at low scanning rates (almost hemi-spherical diffusion layer) and as a macroelectrode at high scanning rates (planar semi-infinite diffusion layer), in the latter case shows a behaviour similar to that already discussed for electrodeposited Ag disks, although at far higher scan rates v.

Figure 9 presents the CVs recorded at 2,000 mV s^{-1} at different trichloromethane concentrations. In this case the two groups of peaks, 1 and 2, are also clearly present. The more substantial differences with the electrodeposited Ag electrodes are: (i) the general positive shift of peak potential; (ii) the contraction of group 1 into one large peak; (iii) the multiplicity of peaks observed for group 2 at increasing $CHCl_3$ concentration; (iv) preservation of the whole characteristics with cycling (not shown in the figure).

In particular, group 1 shifts negatively with increasing concentration. As already observed for Ag deposits on Pt, this is likely due to the coexistence of a multiplicity of reacting sites, and to the saturation of the more active ones, whose features are eventually masked by the increasing characteristics of the less accessible ones. Similar behaviour is observed for group 2. However, in this case two/three peaks are increasingly discernible at increasing $CHCl_3$ concentration. The contraction of group 1 suggests the presence of reactivity sites on the silver powder, whose activity is markedly higher than the 1b sites. Apparently sites 1a are absent, possibly because the powder is not freshly prepared. Nonetheless, the powder exhibits high electroreductive properties, very likely due to its morphology. As expected, lowering the scanning rate leads to a progressive modification of the CV shapes.

Figure 10 reports the CVs recorded at 100 mV s^{-1} for the same substrate concentrations presented in Fig. 9. The overall characteristics resemble that predicted for a

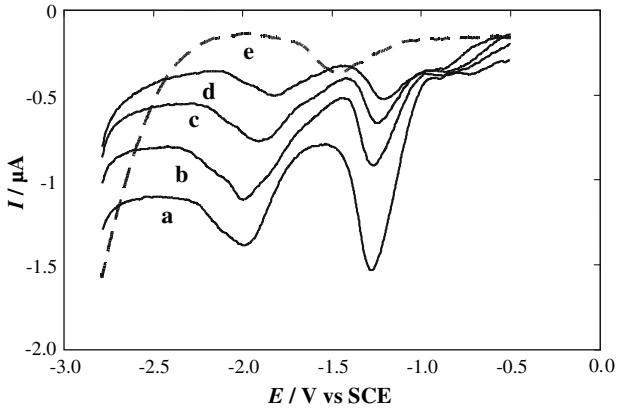

Fig. 9 CV characteristics (1st cycle) of Ag_powder, in TEATFB 0.1 M in MeCN, $v = 2{,}000$ mV s^{-1}, containing $CHCl_3$ at (a) 6.7 mM, (b) 4.2 mM, (c) 2.5 mM, (d) 1.3 mM. Line (e) represents background electrolyte. The reverse scan has been omitted for the sake of clarity

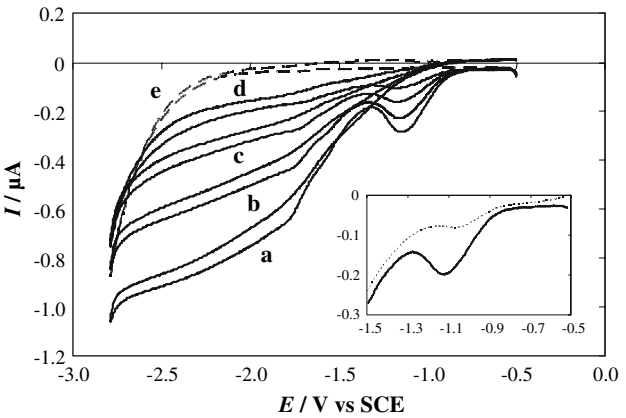

Fig. 10 CV characteristics (1st cycle) of Ag_powder, in TEATFB 0.1 M in MeCN, $v = 100$ mV s^{-1}, containing $CHCl_3$ at (a) 6.7 mM, (b) 4.2 mM, (c) 2.5 mM, (d) 1.3 mM. Line (e) represents background electrolyte. Inset: forward scan, 1st and 2nd cycle, 6.7 mM $CHCl_3$, the reverse scan has been omitted for the sake of clarity

microelectrode, since the high electronic conductivity of the powder strongly reduces the current penetration depth. Therefore, all the phenomena generate waves, with the exception of that giving rise to the first peak in the first cycle. We suggest that this peak is due to reduction of trichloromethane present inside the cavity at the beginning of the experiment, an amount that is consumed during the first scan. In the subsequent cycles, when no trichloromethane (or a negligible quantity) is present inside the cavity, the electrode starts to behave as a silver microdisk of rather high surface roughness, and the peak is replaced by a small sigmoidal wave (see Fig. 10 inset), so that at least three consecutive waves are discernible.

The dependence on trichloromethane concentration is reported in Fig. 11 for the I_{peak} at around −1.1 V and for the I_{wave} at −1.8 V. In both cases the observed excellent

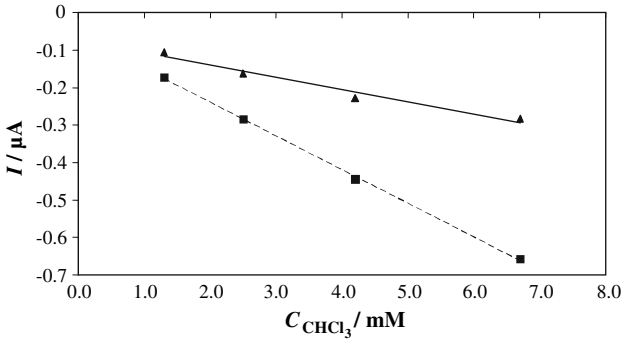

Fig. 11 I vs. c_{CHCl_3} characteristics from data in Fig. 10: (triangles) I_{peak} at −1.1 V; (squares) I_{wave} at −1.8 V. Lines represent the interpolating linear regressions

linear behaviour highlights the applicability of C-ME supported Ag powders to quantitative determinations of volatile halocompounds. In this context, the reproducibility limits observed in filling the cavity are more than balanced by the advantage of working with an easily and quickly refreshable electrode, thus overcoming the problem of the rapid aging of the sensing Ag surface.

4 Discussion

The electroreductive hydrodehalogenation of organic halides follows the general stoichiometry [25]:

$$R - X + 2e^- + H^+ \rightarrow R - H + X^- \quad (2)$$

which applied to the trichloromethane case corresponds to:

$$CHCl_2Cl + 2e^- + H^+ \rightarrow CHCl_2H + Cl^- \quad (3)$$

with formation of dichloromethane.

Reaction (3) can be repeated using di- or mono-chloromethane as reactant, ultimately leading to methane. On the whole, a separate voltammetric peak could be expected for each dechlorination step.

On this basis, as already observed in a previous work [9], the 1st group of peaks in the −1.2/−1.6 V region (−1.1/−1.3 V on silver powders) should be related to hydrodehalogenation of trichloromethane to dichloromethane, while the 2nd group of peaks around −2 V should correspond to the formation of chloromethane, since the reduction of dichloromethane is observed in the same potential zone [9]. Nonetheless, preparative electrolysis experiments performed at controlled potentials between −1.2 and −1.6 V [9, 10] gave methane as final product, thus pointing to a possibly different reaction pathway.

Consequently, the presence of a multiplicity of peaks could either suggest (as already assumed in [9, 10]) the coexistence of sites of different activity, or the presence of multiple reaction steps. The use of the C-ME has disclosed

the coexistence of at least three peaks (at high scanning rates) even for group 2, a feature not observed on the electrodeposited disk electrodes.

5 Conclusions

The responses described in the previous sections on three different kind of electrodes highlight the dependence of the voltammetric behaviour and, in turn, of the electrocatalytic activity, on the silver surface, the micro-sized silver powders showing the highest performances, as inferred from the less negative potential values. This gain in the reduction potentials observed on the C-ME, and the multiplicity of peaks around −2 V also suggest that the expulsion of the third Cl substituent becomes accessible. This result suggests the possibility that, on extremely active sites, the reduction of trichloromethane proceeds to complete hydrodehalogenation at potentials well above (less negative than) −2 V.

The use of powders allows the setting up of three-dimensional electrodes, a feature especially interesting when treating large volume of dilute solutions. Gas diffusion electrodes could be applied to the treatment of low conducting media. In all cases, supporting silver micro- or nano-particles onto a dispersed matrix (e.g. carbon) would enable substantial saving in both energy and materials.

Acknowledgements The authors thank Professor Salvatore Daniele, University of Venice—Department of Physical Chemistry, for fruitful discussions. The authors also acknowledge Stephan Borensztajn (CNRS—UPR 15) and Dr. Benedetta Sacchi (UMIL—DCFE) for SEM analysis. Financial support of COST (Chemistry Working Group—COST action D29—WG-0006/03: Green Organic Electrochemistry), MUR-The University of Milan (FIRST funds) and Fondazione Monte dei Paschi di Siena are gratefully acknowledged.

References

1. Papp R (1996) Pure Appl Chem 68:1801
2. Chen G (2004) Sep Purif Techol 38:11
3. Rondinini S, Mussini PR, Sello G, Vismara E (1998) J Electrochem Soc 145:1108
4. Rondinini S, Mussini PR, Crippa F, Sello G (2000) Electrochem Commun 2:491
5. Rondinini S, Mussini PR, Muttini P, Sello G (2001) Electrochim Acta 46:3245
6. Rondinini S, Mussini PR, Specchia M, Vertova A (2001) J Electrochem Soc 148:D102
7. Doherty AP, Koshechko V, Titov V, Mishura A (2007) J Electroanal Chem 602:91
8. Isse AA, Ferlin MG, Gennaro A (2005) J Electroanal Chem 581:38
9. Rondinini S, Vertova A (2004) Electrochim Acta 49:4035
10. Fiori G, Rondinini S, Sello G, Vertova A, Cirja M, Conti L (2005) J Appl Electrochem 35:363
11. Valette G, Hamelin A, Parsons R (1978) Z Phys Chem Neue Fol 113:71
12. Foresti ML, Innocenti M, Forni F, Guidelli R (1998) Langmuir 14:70086
13. Mussini PR, Ardizzone S, Cappelletti G, Longhi M, Rondinini S, Doubova LM (2003) J Electroanal Chem 552:213
14. Migani A, Illas F (2006) J Phys Chem 110:11894
15. Ardizzone S, Cappelletti G, Mussini PR, Rondinini S, Doubova LM (2003) Russ J Electrochem (translation of Elektrokhimija) 39:170
16. Miranda-Hernandez M, Gonzalez I,Batina N (2001) J Phys Chem B 105:4214
17. Isse AA, Gottardello S, Maccato C, Gennaro A (2006) Electrochem Commun 8:1707
18. Zheng J, Li X, Gu R, Lu T (2002) J Phys Chem B106:1019
19. Vivier V, Cachet-Vivier C, Wu BL, Cha CS, Nedelec J-Y, Yu LT (1999) Electrochem Solid-State Lett 2:385
20. Cachet-Vivier C, Vivier V, Cha CS, Nedelec J-Y, Yu LT (2001) J Electrochem Soc 148:E177
21. Cachet-Vivier C, Vivier V, Cha CS, Nedelec J-Y, Yu LT (2001) Electrochim Acta 47:181
22. Vivier V, Cachet-Vivier C, Nedelec J-Y, Yu LT, Joubert J-M, Percheron-Guégan A (2003) J Power Sources 124:564
23. Bozzini B, Mele C, Romanello V (2006) J Electroanal Chem 592:25
24. Bond AM, Luscombe D, Oldham K, Zoski CG (1988) J Electroanal Chem 249:1
25. Costentin C, Robert M, Savéant J-M (2006) Chem Physics 324:40